NON-GIMBALED ANTENNA POINTING

BY

JEANNINE S. VIGIL, B.S.

A Thesis submitted to the Graduate School

in partial fulfillment of the requirements

for the Degree

Master of Science in Electrical Engineering

New Mexico State University

Las Cruces, New Mexico

August 1997

"Non-Gimbaled Antenna Pointing," a thesis prepared by Jeannine S. Vigil in partial fulfillment of the requirements for the degree, Master of Science in Electrical Engineering, has been approved and accepted by the following:

Timothy J. Pettibone
Dean of the Graduate School

Stephen Horan
Chair of the Examining Committee

Date

Committee in charge:

Dr. Stephen Horan, Chair

Dr. Sheila B. Horan

Dr. Reinhard Laubenbacher

Dr. James P. LeBlanc

ACKNOWLEDGMENTS

I would like to thank Dr. Stephen Horan, my thesis advisor, for all his help and patience towards the completion of my research. I am especially grateful to Dr. Sheila Horan for her guidance and advice during my graduate career. I extend my appreciation for this research, sponsored by the National Aeronautics and Space Administration through grant NAG 5-1491 to New Mexico State University. And to my close friend, Piyasat Nilkaew, who was always willing to help.

Most of all, I would like to thank my family for giving me support, love and guidance to reach for my goals, I am forever indebted to you. To all my friends, thanks for listening and telling me never to give up. You have made my college career memorable.

VITA

[redacted]—Born in [redacted]

1990—Graduated from Espanola Valley High School, Espanola, New Mexico

1995—B.S. Degree in Electrical Engineering from New Mexico State University

1996-1997—Graduate Research Assistant by a grant from the National Aeronautics and Space Administration (NASA) #NAG 5-1491, Manuel Lujan Jr. Space Tele-Engineering Laboratory in the Klipsch School of Electrical and Computer Engineering Department, New Mexico State University

PROFESSIONAL AND HONORARY SOCIETIES

Society of Hispanic Professional Engineers

Order of the Engineer

Sociedad de Ingenieros

PUBLICATIONS

Stephen Horan and Jeannine Vigil, "Further Results For Non-Gimbaled Antenna Pointing", Technical Report Series, NMSU-ECE-96-018, December 1996.

FIELD OF STUDY

Major Field: Electrical Engineering with an emphasis in Telecommunications

NON-GIMBALED ANTENNA POINTING

Jeannine S. Vigil

NMSU-ECE-97-019 August 1997

ABSTRACT

NON-GIMBALED ANTENNA POINTING

BY

JEANNINE S. VIGIL, B.S.

Master of Science in Electrical Engineering

New Mexico State University

Las Cruces, New Mexico, 1997

Dr. Stephen Horan, Chair

The small satellite community has been interested in accessing fixed ground stations for means of space-to-ground transmissions, although a problem arises from the limited global coverage. There is a growing interest for using the Space Network (SN) or Tracking and Data Relay Satellites (TDRS) as the primary support for communications because of the coverage it provides. This thesis will address the potential for satellite access of the Space Network with a non-gimbaled antenna configuration and low-power, coded transmission.

The non-gimbaled antenna and the TDRS satellites, TDRS-East, TDRS-West, and TDRS-Zone of Exclusion, were configured in an orbital analysis software package called Satellite Tool Kit to emulate the three-dimensional position of the satellites. The access potential, which is the average number of contacts per day and the average time per contact, were obtained through simulations run over a 30-day period to gain all the possible orientations. The orbital altitude was varied from 600 km through 1200 km with the results being a function of orbital inclination angles varying from 20° through 100° and pointing half-angles of 10° through 40°.

The communication performance was estimated over the range of small satellite missions by considering the 50th percentile, which NASA estimates that the daily volume generated in these missions is 864,000,000 bits per day. As the analysis indicated, the data rates for the simulation models supported the 50th percentile level as a function of contact duration, which implies that the throughput will be 864,000,000 bits per day. The 50th percentile level can be achieved by using a wide half-angle and a single TDRS or a narrow half-angle antenna and the full constellation. Considering above the 50th percentile indicated a link penalty of approximately 35 dB, which might not be applicable in some cases. Therefore, this study concentrated on the 50th percentile.

To compare the validity of the simulations, Jet Propulsion Laboratory granted the use of the TOPEX satellite. The TOPEX satellite was configured to emulate a spin-stabilized antenna with its communications antenna stowed in the zenith-pointing direction. This mimicked the antenna pointing spin-stabilized satellite in the simulations. To make valid comparisons, the TOPEX orbital parameters were entered into Satellite Tool Kit and simulated over five test times provided by Jet Propulsion Laboratory. The indications were significant in that the relative signal strengths from the simulations and the actual experiment were similar. This was an indication that the simulation methodology was accurate when tested against an actual test experiment.

Based on the simulations and actual test results, the use of non-gimbaled antennas to access the Space Network has a significant advantage over fixed ground stations.

TABLE OF CONTENTS

LIST OF TABLES

LIST OF FIGURES

ACRONYM AND SYMBOL LIST

BER	Bit Error Rate
C/N_o	Carrier-to-Noise Power Ratio
dB	Decibels
ECF	Earth-Center Fixed
EIRP	Effective Isotropic Radiated Power
HPBW	Half Power Beam Width
JPL	Jet Propulsion Laboratory
LEO	Low Earth Orbit
MA	Mean Anomaly
MM	Mean Motion
MSGP4	Merged Simplified General Perturbations
NASA	National Aeronautics and Space Administration
RAAN	Right Ascension of the Ascending Node
SN	Space Network
STK	Satellite Tool Kit
TDRS	Tracking and Data Relay Satellite
TDRS-E	TDRS-East
TDRS-W	TDRS-West
TDRS-ZOE	TDRS-Zone of Exclusion

UT	Universal Time
WSC	White Sands Complex
λ	Wavelength (m)
ω_p	Argument of Perigee

CHAPTER 1 - INTRODUCTION

Man-made satellites have been known to have an unprecedented capability for accessing fixed ground stations and establishing communications links to transmit their data from space to ground as in Figure 1. These communication links only allow transmission when the satellite is above the local horizon of the receiving station. This implies that in this mode, communications with the fixed ground station are not continuous but periodic throughout the day. For example, Figure 2 illustrates a 30-day simulation of a satellite accessing ground stations using a 28.5° orbital inclination angle, a 600-km altitude, and a 20° half angle for a spin-stabilized satellite's antenna field of view. Three fixed ground stations located at latitudes of 32.5° N (White Sands Complex), 21.6° N (Hawaii), and 64.3° N (Alaska) were used. The highlighted regions centered on each fixed ground station antenna shows the opportunities along the spin-stabilized satellite's ground tracks when the satellite can access each fixed ground antenna. The results shown in Table 1 indicate that a satellite in a 600-km altitude orbit communicating with a fixed ground station at 32.5° N would typically have 6.6 contacts per day with an average duration of 11.25 minutes for a total contact time of 74.22 minutes per day when the orbital inclination angle is 28.5°. When the orbit is sun-synchronous, the same satellite and ground station configuration would have 5 contacts per day at 10.15 minutes per contact for a total contact time of 50.76 minutes. The results in Table 1 also indicate that the fixed ground station at 64.3° N (Alaska), is not visible to a satellite with an orbital inclination of 28.5°,

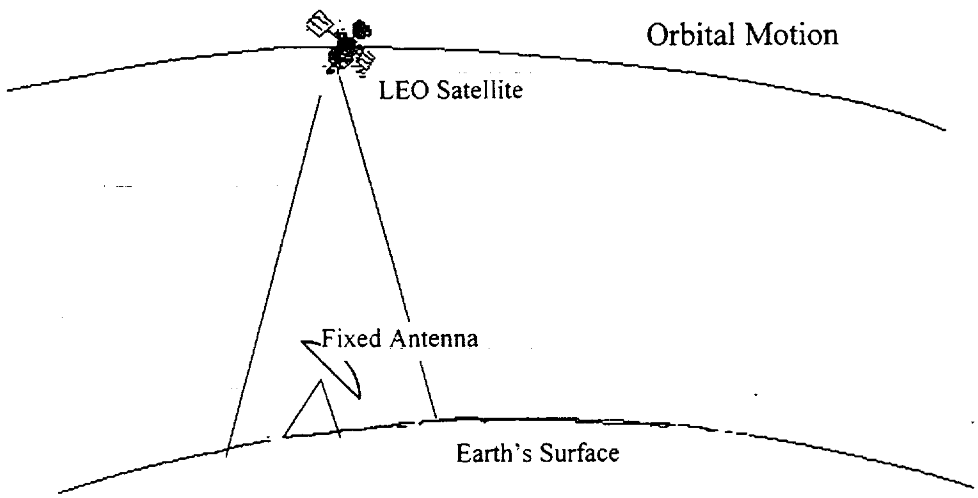

Figure 1. Spinning Satellite Accessing a Fixed Ground Station (Not To Scale)

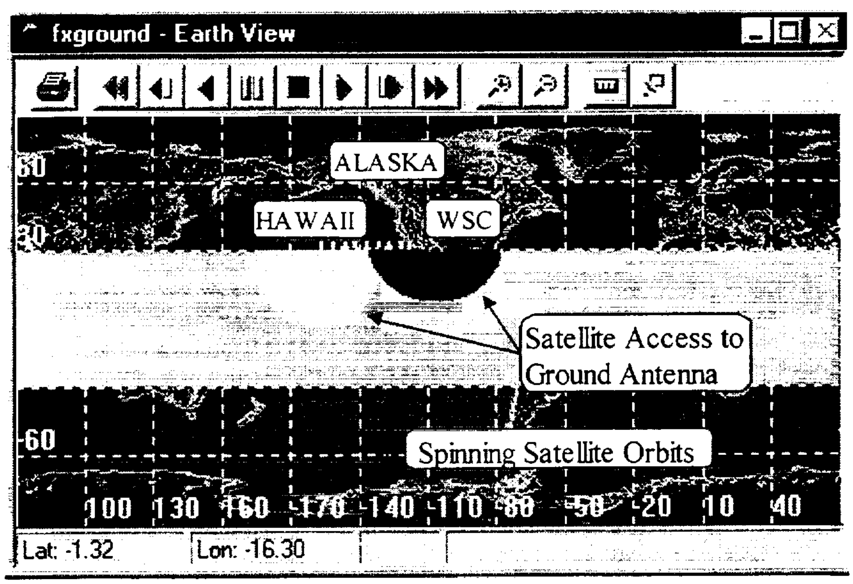

Figure 2. Ground Tracks For Full 30-day Simulation Period Using 28.5° Orbital Inclination Angle, a 600-km Orbital Altitude, and a 20° Half-Angle Field of View

Table 1. Average Contacts Per Day and Average Contact Duration for Fixed Ground Stations

	32.5° N (WSC)		21.6° N (HAWII)		64.3° N (ALASKA)	
	Orbital Inclination		Orbital Inclination		Orbital Inclination	
	28.5°	Sun-Synchronous	28.5°	Sun-Synchronous	28.5°	Sun-Synchronous
Min (sec)	57.48	148.40	102.93	76.64	Satellite	8.48
Max (sec)	805.09	764.90	817.45	764.59	Not Visible	771.54
Mean (sec)	674.73	609.06	725.28	595.68		628.33
Total Duration (sec)	133596.14	91359.02	174792.03	82203.36		215517.11
Total Duration (min)	2226.60	1522.65	2913.20	1370.06		3591.95
Contact Time (sec)	4453.20	3045.30	5826.40	2740.11		7183.90
Contact Time (min)	74.22	50.76	97.11	45.67		119.73
Number of Contacts	6.60	5.00	8.03	4.60		11.43
Contact Duration (sec)	674.73	609.06	725.28	595.68		628.33
Contact Duration (min)	11.25	10.15	12.09	9.93		10.47

but is visible for a satellite in a the sun-synchronous orbital inclination. This fixed ground station shows that there is 11.43 contacts per day with a total average duration of 10.47 minutes. Generally, these terminals typically provide up to 12 minutes of coverage during an orbit that is within the visibility of the ground station, however, not all orbits will pass over the ground station so that coverage gaps will exist in the data flow.

In order to overcome the limited visibility due to latitude and orbital inclination angle effects and to obtain a more global coverage one would need to construct a network of fixed ground stations. As an alternative to this, the Space Network (SN), operated by the National Aeronautics and Space Administration (NASA), has been designed to transmit data to and from satellites using the Tracking and Data Relay Satellites (TDRS). The TDRS are in a geostationary orbit and interface to the White Sands Complex (WSC) in New Mexico for the data ground entry point [1]. A significant advantage of the SN over a fixed ground station is that all low-earth satellite orbits will be within the visibility area of at least one of the TDRS within the SN for a large part if the orbit. The potential exists to establish a communications link between the orbiting satellite and ground communications networks whenever the user satellite can point an antenna in the direction of any one of the TDRS satellites. The SN also avoids the cost of operation and maintenance of fixed ground stations.

While the SN has cost and access advantages, the SN has not been frequently considered by developers of small satellites because of perceived problems in scheduling communications and the cost in weight and power to use gimbaled, directional antennas for the communications support. There is also a significant communications link power penalty for going to a low-earth orbit (LEO) first rather than directly to a ground station. This thesis addresses the potential for SN access using non-gimbaled antennas in the design of the small satellite using modest transmission power to achieve the necessary space-to-ground transmissions. This class of satellite needs low-cost data transmission as well as low-cost construction. The simulations and analysis will illustrate how a modest satellite configuration can be used with the SN to achieve the data transmission goals of a number of users and thereby rival the performance achieved with fixed ground stations.

1.1 Space Network Background

The Space Network is composed of three active TDRS satellites located at -174°, -41°, and +85° longitude and denoted as TDRS-West, TDRS-East, and TDRS-ZOE to close Zone of Exclusion over the Indian Ocean, respectively. Each TDRS can support K-band (KSA) and S-band single access (SSA) communications and S-band multiple access communications (SMA) [2]. The choice of the TDRS to be used on a given data service depends on the relative satellite positions, the availability of communications links, and the requested service duration. The data link between the SN and the ground communications networks is run through the WSC facility which interfaces with the user satellite's control center utilizing NASA's communications links. Presently, the S-band multiple access (SMA) service has the greatest probability of availability to the small satellite user so it was used in the data throughput analysis. The SMA service uses code division multiplexing with each user having a return carrier frequency of 2287.5 MHz [3]. Figure 3 illustrates the TDRS locations and a sample of user satellite orbits over a 24-hour period. From the figure, all the corresponding TDRS are represented as small rectangular boxes at their designated locations with the orbits given over a 24-hour time period.

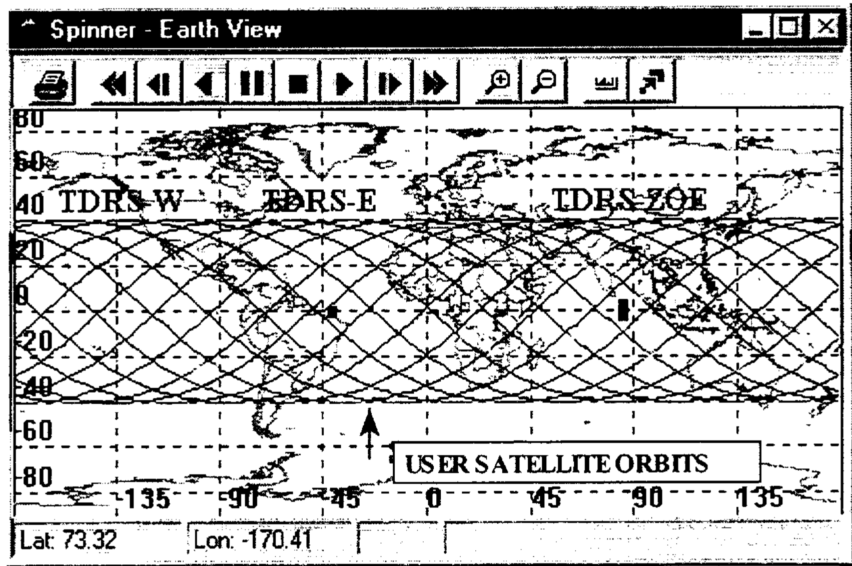

Figure 3. Example Orbital Ground Tracks for the Three TDRS Satellites and the Spinning Satellite over a 24-hour period Using STK to Perform the Simulation

1.2 Small Satellite Profile

For the conceptual design of a small satellite system, the following assumptions are made as a representative operational baseline:

1. the communications subsystem is able to supply radiated output power in the range of 10 Watts
2. the antenna system can provide a minimum gain of 5 dB
3. the antenna system is surface mounted along a radial vector connecting the satellite with the center of the earth and pointing away from the center of the earth
4. the satellite is spin-stabilized with a nadir orientation; the long axis of the spacecraft is along the radial vector connecting the satellite with the center of the earth

5. satellite contact between the small satellite and the SN can be initiated as the small satellite sweeps past a TDRS position in its orbit
6. the SN S-Band Multiple Access (SMA) service can be used for the communications link; this implies that the TDRS is capable of tracking the satellite using open-loop techniques.
7. the spin-stabilized satellite is given orbital elements corresponding to an orbital altitude between 600 km and 1200 km in increments of 200 km
8. the orbital inclination angle of interest will lie between 20° and 100°
9. the antenna cone angle of interest will lie between 10° and 40° corresponding to effective half-power beamwidths of 20° through 80°.

The orbital elements for the spin-stabilized satellite, Right Ascension of Ascending Node, Argument of Perigee, and Mean Anomaly, are set to 0° in the simulations since the only interest is the determination of the general access characteristics, not the position of a real satellite.

The conceptual idea for using these conditions is to have a range of orbital parameters so that small satellite users will have a variety of choices in the design specifications.

1.3 Communication Performance

So far, we have only considered the pointing geometry for the access to the SN. To determine the actual communications performance, we need to also examine the effects of the orbit on the link power budget. This thesis will concentrate on the return data link (user satellite through TDRS to the ground). The forward command link (ground through TDRS to the user satellite) will usually be a lower data rate service and the data volume will also typically be considerably lower than the return link's requirements. Therefore, the assumption is made that if the return link requirements are satisfied, then the forward link requirements can also be satisfied.

The link budget analysis is relatively straightforward and is outlined below [4]. Let us begin with a transmit antenna that radiates isotropically in free space at a power level of P_T watts. The power density at a distance d from the antenna is $P_T/4\pi d^2$ W/m^2. If the transmitting antenna has some particular direction, the power density in that direction is increased by a factor called the antenna gain and denoted G_T. In such a case, the power density at distance d is $P_T G_T/4\pi d^2$ W/m^2. The product $P_T G_T$ is usually called the effective radiated power (EIRP).

A receiving antenna pointed in the direction of the radiated power gathers a portion of the power that is proportional to it cross-sectional area. Hence, the received power extracted by the antenna may be expressed as

$$P_R = P_T G_T A_R/4\pi d^2 \qquad (1)$$

where A_R is the effective area of the antenna. The basic relationship between the gain G_R of an antenna and its effective area is

$$A_R = G_R \lambda^2/4\pi m^2 \qquad (2)$$

where λ=c/f is the wavelength of the transmitted signal, c is the speed of light (3 x 10^8 m/s), and f is the frequency of the transmitted signal.

If we substitute (2) for A_R into (1), we obtain an expression for the received power in the form

$$P_R = P_T G_T G_R/(4\pi d/\lambda)^2 \qquad (3)$$

The factor

$$L_S = (\lambda/4\pi d)^2 \qquad (4)$$

is called the free-space loss [5].

With the basic concepts of a link budget analysis, the effects of antenna patterns and space loss on a received signal strength (C/N_o) can be investigated as a function of the small variations in the pointing during a pass. The variation in the received signal power due to the link distance is normally computed in the link power budget by the space loss term. The definition for the space loss, L_s, is given in equation (4), but *in dB,* is given by

$$L_s = 20\log(4\pi R/\lambda) \quad \text{dB} \qquad (5)$$

where R is the link range and λ is the operating wavelength. To compute the power variation relative to that at the minimum range, R_o, the relative space loss, L_{sr}, is computed using

$$L_{sr} = 20\log(R/R_o) \quad \text{dB} \qquad (6)$$

The link range, R, will vary over the contact time due to the orbital motion of the satellite.

The antenna pattern variation in the user satellite can be computed using an assumed tapered parabolic feed for the antenna. Under this assumption, the normalized gain pattern or pointing loss in dB units as a function of the off-axis pointing angle, θ, is given by

$$L_p = 10\log[64|J_2(u)/u^2|^2] \qquad (7)$$

where $u = \pi D \sin(\theta)/\lambda$, D is the antenna diameter, and λ is the operating carrier wavelength [6] [7]. The predicted variation in the received signal strength is therefore based on the addition of the space loss and antenna pattern loss in dB units over time.

For this study, the path loss and antenna gain differential results in approximately 35 dB power difference between a data link to TDRS versus a ground station using the SMA service. This relative link penalty was computed by the ratio of the maximum slant range from the user satellite to the TDRS satellite, approximately 35,000 km and the minimum altitude of 600 km, thus

$$L_{SR} = 20\log(35000 \text{ km}/600 \text{ km}) = 35 \text{ dB}.$$

While this is a significant link penalty, we will investigate the potential for users with low data volumes to be transmitted each day, this link penalty can be overcome and produce usable communications.

This thesis will address the potential for satellite access of the Space Network with a fixed antenna configuration and low-power, coded transmission. We believe that the fixed antenna pointing case investigated here will show that there will be a sufficient number of contacts per day with sufficient total duration to support the data communications needs of a small satellite mission. For this class of users, using the modest configuration given earlier, there will be the possibility to transmit the required data volume. In Chapter 2, we will see how the commercially-available simulation package Satellite Tool Kit is used to simulate the orbits of a spin-stabilized satellite and the three TDRS satellites over a 30-day period to determine the potential access times and durations. Associated with the access information is the determination of the slant path between the spin-stabilized satellite and each TDRS. Chapter 3 will discuss the TOPEX experiment and the basic analysis work to generate five test passes to help verify the simulation results. In Chapter 4, the results will be explained for the simulation models and the actual test experiment with TOPEX. Chapter 5 will give an overview of the analysis done to determine the data rate and data throughput. Lastly, Chapter 6 will provide the conclusions drawn from the study.

CHAPTER 2 - DETERMINING ORBITAL ACCESS

A series of simulations using the software package Satellite Tool Kit (STK) [8] were performed to determine the access potential for a simple satellite communications system. The access potential is determined by considering the average number of contacts per day, the average time per contact at each TDRS satellite, and the average time per contact through the constellation of three TDRS satellites. From the measures, we can estimate an average total daily contact time on a per-satellite basis and a whole constellation basis. The simulations were configured to predict the three-dimensional positions of all three TDRS and a spin-stabilized satellite with a zenith-pointing antenna. The purpose for using the Satellite Tool Kit package included gravitational perturbation models for propagating the orbital elements over the simulation period (STK used the MSGP4 propagation model for all the simulations run here) and it had the ability to choose the attitude control system model for the satellites.

2.1 Models Simulated

To investigate the potential access during a 30-day period, the parameters for the spin-stabilized satellite were simulated over the following conditions:

a. the spin-stabilized satellite was given orbital elements corresponding to an orbital altitude between 600 km and 1200 km in increments of 200 km
b. the orbital inclination angle was varied from 20° through 100° in increments of 20°

c. the antenna cone angle of 10° through 40° in increments of 10° was used corresponding to the effective beam widths of 20° through 80°.

The simulations were performed in a combination of orbital inclination angle and antenna field of view over an orbital altitude.

The 30-day simulation period was chosen because over that time frame, all orientation differences between the TDRS and spinning satellite are observed. Durations longer than this do not significantly change the average results while simulations much shorter than this duration miss many potential configuration states. The orbital parameter ranges were chosen based on discussions with NASA and looking at typical mission profiles.

2.2 Configuring Satellite Tool Kit for Simulations

Selecting the "Basic Properties" window in STK, Figure 4, allows the user to also select the earth gravity model propagator, MSGP4 (Merged Simplified General Perturbations). The MSGP4 propagator is used for gravitational effects and uses the two-line mean orbital element set taken from [9] and listed in Table 2, for the corresponding TDRS. The mean orbital elements are explained below:

Element	**Description**
SSC Number	This specifies the catalog number of the spacecraft as listed in the 2-line element set.
Orbit Epoch	This specifies the data and time that the specified orbit elements are true. This

	format is YYDDD.DDDDDDDD.
Mean Motion	This specifies the number of revolutions per day for the orbital period.
Eccentricity	This describes the shape of the ellipse. A value of 0 represents a perfectly circular orbit; a value of 1 represents a parabolic path.
Inclination	This is the angle between the angular momentum vector (perpendicular to the plane of the orbit) and the intertial Z axis
Argument of Perigee	This is the angle from the ascending node to the eccentricity vector (lowest point of orbit) measured in the direction of the satellite's motion. The eccentricity vector points from the center of the Earth to perigee with a magnitude equal to the eccentricity of the orbit.
Right Ascension of the Ascending Node	This is the angle from the inertial X axis to the ascending node. The ascending node is the point where the satellite passes through the inertial equator moving from south to north. Right ascension is measured as a right-handed

	rotation about the inertial Z axis and is referenced to the Vernal Equinox.

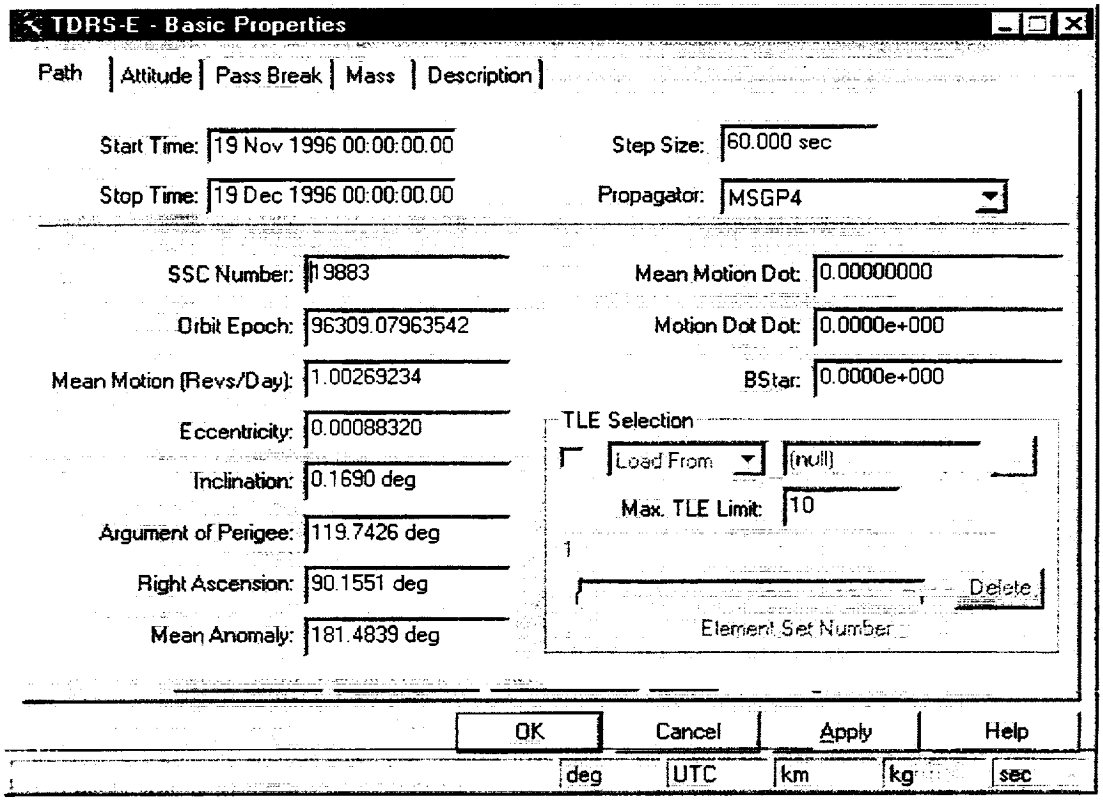

Figure 4. "Basic Properties" Window In Satellite Tool Kit For TDRS-East

To visualize these orbital parameters, Figure 5 depicts the inertial coordinate system and the orbital elements.

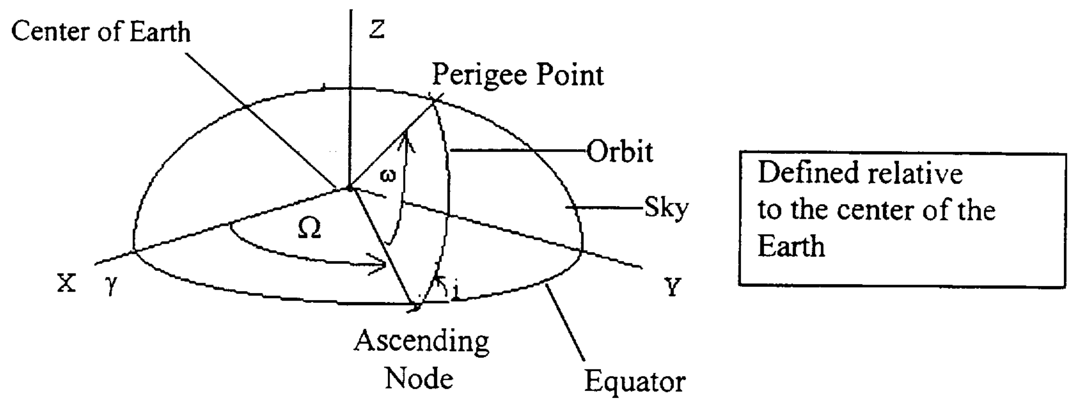

i = inclination angle
ω = argument of perigee
Ω = right ascension of ascending node (RAAN)
γ = Vernal Equinox

Figure 5. Orbital Elements in the Inertial Coordinate System

The attitude control model for all three TDRS was set to the default of nadir alignment with ECF (Earth-Center Fixed) velocity constraint. With the ECF constraint, the orbit track always appears above the ground track.

The antenna systems on the three TDRS were modeled as sensor objects within the simulation. In Satellite Tool Kit, "sensor objects" have a boresight pointing direction and an associated acceptance cone with a user-controlled central angle which defines the sensor field of view. For antennas, this acceptance cone will usually be related to the antenna half-power beamwidth (HPBW). The cone angle used in Satellite Tool Kit would then be one-half of the HPBW as shown in Figure 6.

Table 2. Orbital Elements for the TDRS Spacecraft Used in the STK Simulations			
element	**TDRS-E**	**TDRS-W**	**TDRS-ZOE**
epoch	96309.07964	96309.52072	96310.80323
MM (rev/day)	1.00269234	1.00270108	1.00269
eccentricity	0.0008832	0.0004056	0.0005781
inclination (degrees)	0.169	0.0743	2.7767
ωp (degrees)	119.7426	173.4374	153.3718
RAAN (degrees)	90.1551	80.9672	71.2162
MA (degrees)	181.4839	162.7795	195.285

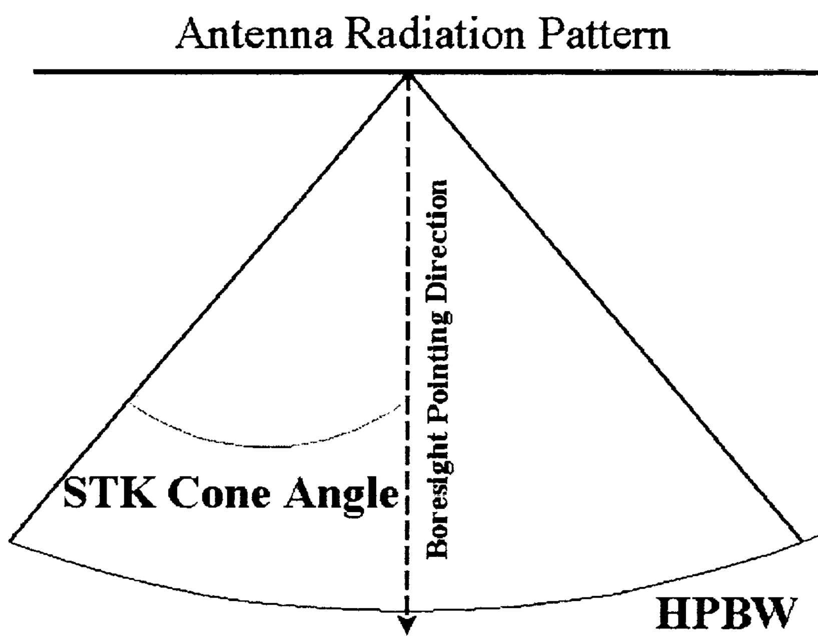

Figure 6. Relationship Between STK Antenna Cone Angle and Antenna HPBW

Contact times between the satellites in the simulation were based upon each being within the acceptance cone of the other for the contact duration. The simulated TDRS was modeled as having an acceptance cone width of +13° corresponding to the actual TDRS MA antenna system pointing range [3].

The spin-stabilized satellite was configured in the same manner as above with the elements shown in Table 3. The orbital elements for the spin-stabilized satellite, Right Ascension of Ascending Node, Argument of Perigee, and Mean Anomaly, were set to 0° since the only interest was the determination of the general access characteristics, not the position of a real satellite. The spin-stabilized satellite was given a fixed antenna pointing towards the local zenith and the antenna's field of view half-angle was varied according to which antenna case was being simulated.

Table 3. Orbital Elements Used for the Spinning Satellite in the STK Simulations

element	value
MM (rev/day)	13.16 through 14.89
Altitude (km)	600 through 1200
eccentricity	0
inclination (degrees)	20° through 100°
ωp (degrees)	0
RAAN (degrees)	0
MA (degrees)	0

With the parameters entered accordingly, Satellite Tool Kit program propagated the orbital elements over the 30-day period for each satellite to account for the perturbations caused by the variations in the gravitational field. In the simulations, an access of a TDRS by the spin-stabilized satellite occurred when the field of view computation indicated that both antenna systems were mutually visible. Figure 7 illustrates that the antenna systems are not mutually visible in position #1 but are visible in position #2. The simulation analysis recorded the start and stop time of each

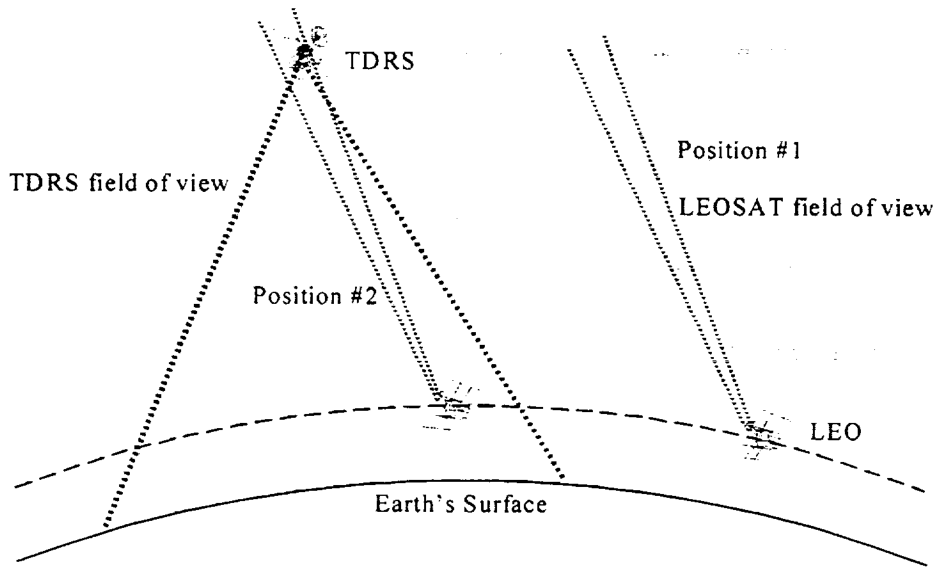

Figure 7. TDRS/Spin-Stabilized Satellite Access Geometry

access period between the spin-stabilized satellite and each TDRS, the pointing angles, and the slant range between the satellites and produced a report listing them over the simulated 30-day duration. In Chapter 4, we will examine the results of the simulations.

CHAPTER 3 - TOPEX EXPERIMENT

Jet Propulsion Laboratory (JPL) in Pasadena, California, in coordination with Goddard Space Flight Center, granted the use of the TOPEX satellite to perform an experiment to verify the satellite antenna pointing concepts developed using simulations. TOPEX, as illustrated in Figure 8 [10], was chosen due to its orbital motion, which could be used to mimic the antenna pointing of a spin-stabilized satellite. TOPEX is not a spin-stabilized satellite but it is nadir-pointing so its communications antenna could be stowed in the zenith-pointing direction to simulate the configuration of a spin-stabilized satellite with a fixed-pointed antenna.

JPL worked through scheduling constraints to determine the appropriate dates and passes to attempt the request of using the TOPEX high gain antenna when it passes "near" and "far" from a TDRS subsatellite point. After several test passes were performed to determine the best configuration parameters for the experiment, a total of 5 communications passes through TDRS-E and TDRS-W over 5 consecutive days was provided by JPL to perform testing and listed below:

PASS	DATE	TDRS	DOY	TIME (UTC)
1	6/23/97	West	174	3:42:30 - 3:55:00
2	6/24/97	East	175	6:54:30 - 7:06:00
3	6/25/97	East	176	7:15:15 - 7:29:00
4	6/27/97	West	178	15:27:30 - 15:40:30
5	6/27/97	East	178	18:15:30 - 18:29:30

Once the experiment was executed over the five day period, the data collected by JPL was sent to NMSU for examination. The data included the receiver signal strength (C/N_0 in dB-Hz) vs. time plots for each of the five passes.

Figure 8. View of TOPEX Satellite

For comparison, STK was configured to approximate the actual TOPEX test pass. The orbital elements were taken from [9] for the TOPEX satellite and for TDRS-E, and TDRS-W satellites, respectively, and entered into STK. Once all the parameters were entered, STK propagated the orbital elements for the same time frame that the experiment was performed. During the simulated test pass, it was expected that as the TOPEX moved along its orbit, it would sweep past the TDRS position and emulate the desired contact profile. A report listing was generated with the slant ranges for each pass and the contact duration. We will discuss the results of these simulations and compare with the actual results in Chapter 4.

CHAPTER 4 - RESULTS

The following sections discuss the results obtained from the simulations and the TOPEX experiment.

4.1 Simulation Results

In each of the computer simulations, the access potential was examined. The following statistics were investigated as a function of orbital altitude, orbital inclination angle, and antenna cone angle:

1. minimum, maximum, and average contact length in minutes to each TDRS
2. total daily contact duration for each TDRS and the SN constellation
3. average number of contacts per day for each TDRS
4. total daily average contact duration

Tables 4 summarizes the results obtained when the simulations covered a 30-day period with an orbital altitude of 600 km. The average contact time and average contact duration time were taken from the STK report listing for the functions of orbital inclination angles and half-angles and entered into a spreadsheet format. As can be seen in Table 4, the average daily contact times and number of contacts are also given. The average daily contact time was obtained by dividing the total contact duration by 30 days. Tables 5 through 7 were obtained in the same manner for orbital altitudes of 800 km through 1200 km in increments of 200 km. Figures 9 and 10 plot the results for TDRS-West illustrating the *average number of contacts per day* and the *average contact duration* from Tables 4 through 7, respectively.

TDRS-East and TDRS-ZOE satellites had very similar results so only TDRS-West is shown. Figure 11 illustrates the *total* SN constellation average daily contact time.

Figure 9. - Average Number of Contacts per Day as a Function of Orbital Altitude, Orbital Inclination Angle, and Antenna Cone Angle for TDRS West

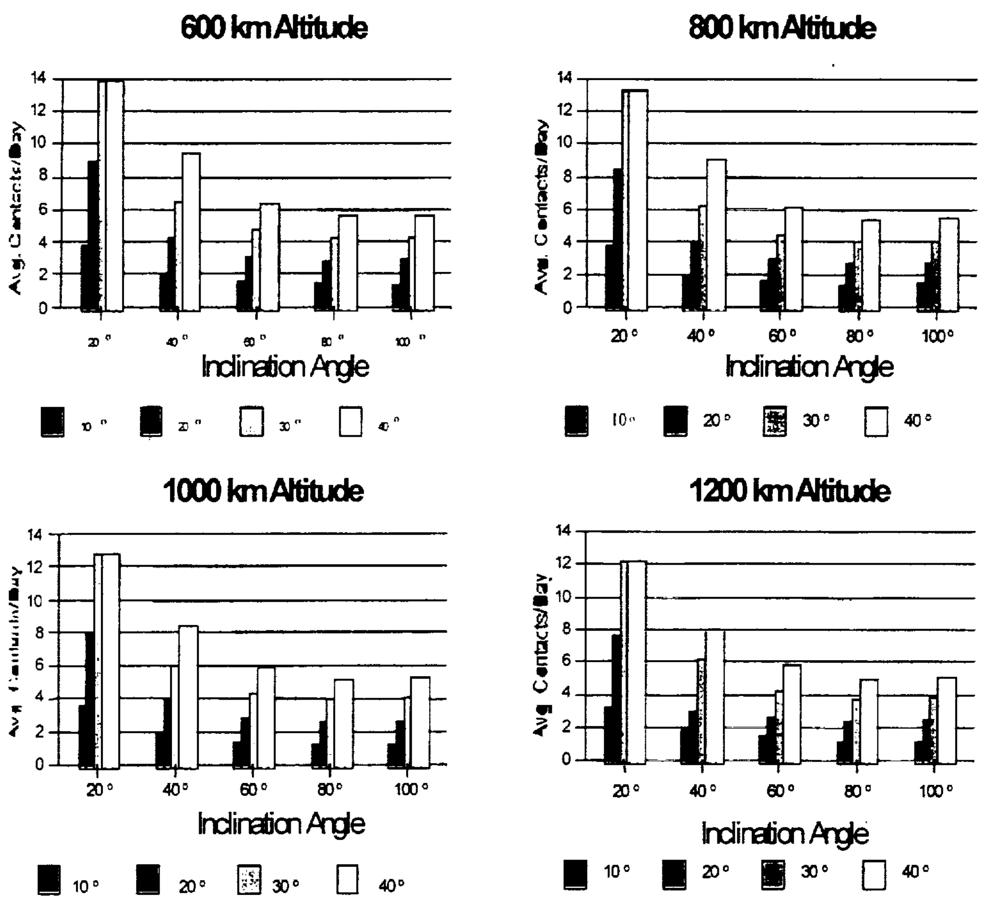

Figure 10. - Average Contact Duration as a Function of Orbital Altitude, Orbital Inclination Angle, and Antenna Cone Angle for TDRS West

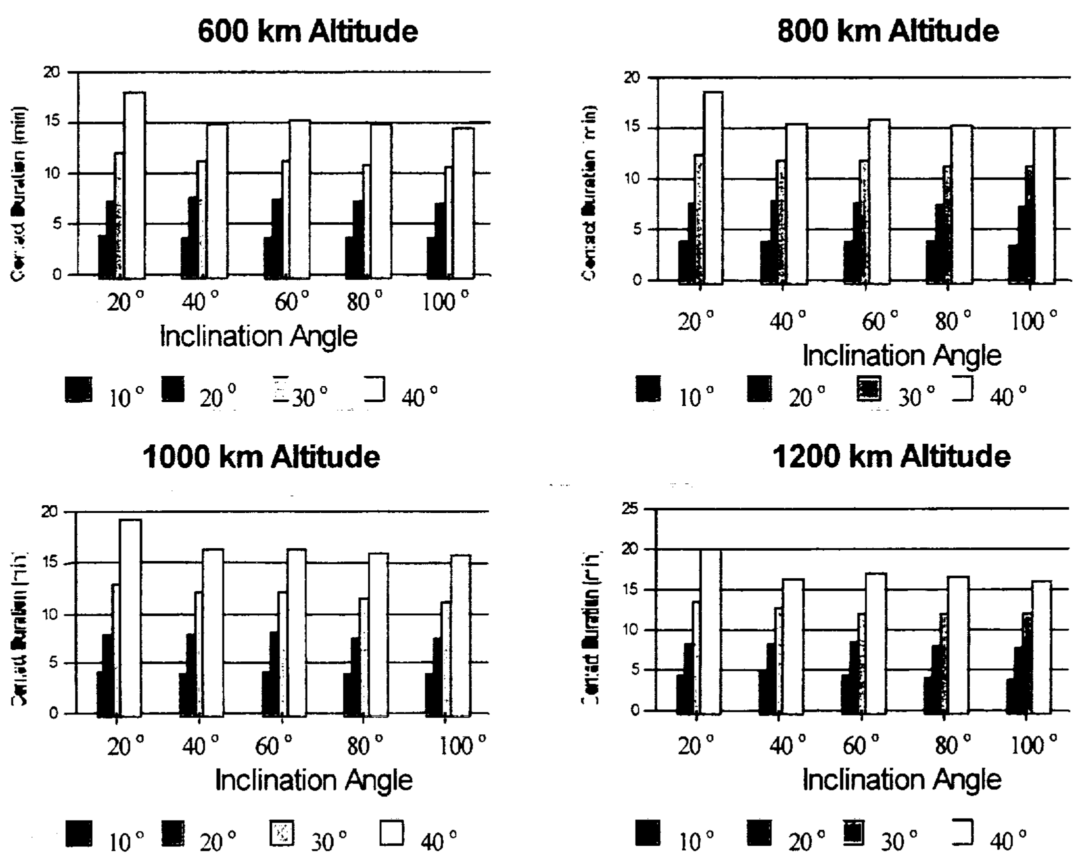

Figure 11. - Total Constellation Average Contact Time as a Function of Orbital Altitude, Orbital Inclination Angle, and Antenna Cone Angle

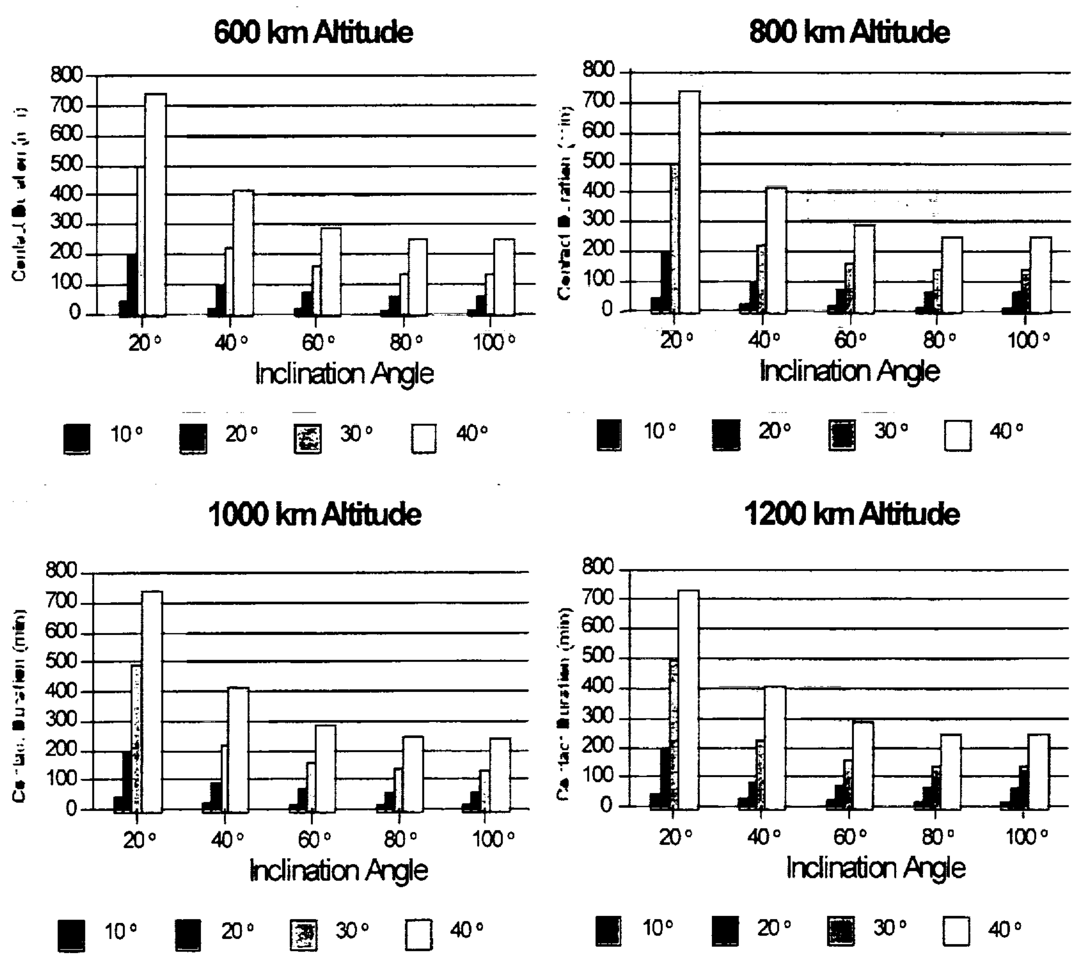

In order for this concept of obtaining average daily contact times and contact durations, the baseline antenna design has to be assumed to have sufficient power that can be obtained from an antenna without steering [10]. This leads to the use of a fairly non-directional antenna system, i.e. one with a large HPBW. The tradeoff with a large HPBW is a low gain for the system thereby giving a low EIRP. Generally, assumptions can be made on which type of antenna will be effective by determining the HPBW and directivity, D. For example, for a typical helical antenna, the HPBW and directivity, D, may be computed from the following equations

$$HPBW = 52^{\circ} / (C/\lambda)(N(S/\lambda))^{1/2} \qquad (8)$$

$$D = 15(C/\lambda)^{2}NS / \lambda \qquad (9)$$

Where C is the helix circumference, N is the number of turns, S is the spacing of the turns, and λ is the radiation wavelength. The available HPBW and gains for the typical helix antennas at the SN S-Band return frequencies were calculated and listed below

	Helix Antenna Performance	
Number of Turns	Gain (dB)	HPBW (degrees)
5	11.3	54.8
10	14.3	38.8
21	17.5	26.8

Based on this study, the non-gimbaled antenna pointing indicated that at least 3 contacts per day were possible with existing technology or realizable antennas, and up to 15 contacts per day were possible with the correct choice of antenna and orbital inclination. The non-gimbaled antenna pointing also gives sufficient contact time through the entire Space Network constellation to make this communication mode reasonable to investigate for actual usage because the antennas are readily available. The technique provides approximately 15 minutes per day at the low end up through several hundred minutes at the high end with the duration being a function of the orbital inclination and antenna HPBW.

The maximum slant paths for the various orbital configurations are plotted against the antenna beamwidths in Figure 12. These maximum slant paths correspond to the start and stop times of the service window. During any satellite service support time, the slant path to a TDRS will vary through the pass and will be minimal at the mid-point of the pass and highest at the end points of the pass (pass start and stop times). As the path becomes shorter, the data rate remaining constant has the effect of reducing the channel bit error rate thereby making the link more reliable in the middle region of the service window.

4.2 TOPEX Results

To compare the validity of the simulations with the actual test measurements, we give the times for the contact over the period of the predicted tests based on the simulations in Table 8.

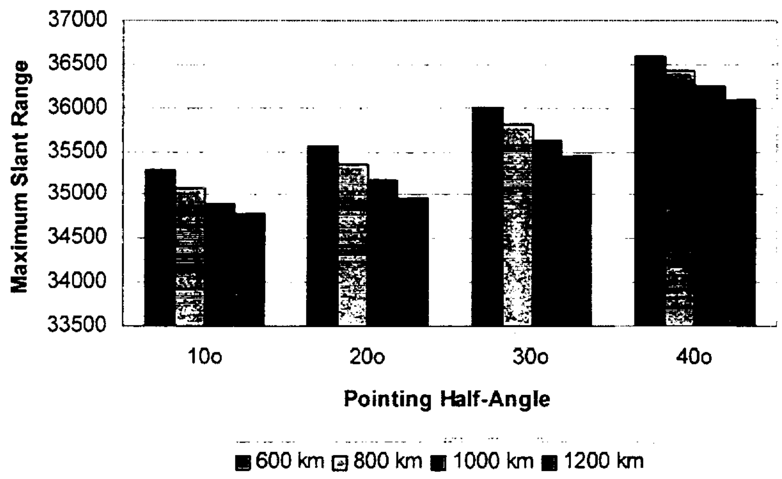

Figure 12. Slant Range as a Function of Antenna Beamwidth

TABLE 8. TOPEX to TDRS Pass Log

		SIMULATED (UT)		PREDICTED (UT)	
TDRS	DAY	START OF PASS	END OF PASS	START TIME	END TIME (UT)
West	174	3:43:42	3:53:13	3:42:30	3:55:00
East	175	6:54:30	7:04:26	6:54:30	7:06:00
East	176	7:16:42	7:26:54	7:15:15	7:29:00
West	178	15:29:00	15:39:28	15:27:30	15:40:30
East	178	18:17:18	18:27:45	18:15:30	18:29:30

This was an indication that the TOPEX configuration in STK was accurate and that our ground procedure for simulating the satellite interactions is valid. A typical ground track for one of the simulated TOPEX passes is shown in Figure 13 with similar results being obtained for the other four passes in the test series in Figures 14 through 17.

From Figure 13, Day 174, the ground track is positioned on the right of TDRS-W, while on Figure 16 Day 178, the ground track is positioned to the left of TDRS-W. In all cases, the five passes were performed to test a variation of patterns with a high gain antenna near a TDRS subsatellite point.

Once the slant ranges were found from the simulations, the relative space loss at the minimum range, R_o, was computed using equation (6). The estimated link range, R, was taken from the simulation for each pass since it varied over the contact time due to the orbital motion of the TOPEX satellite. The antenna pattern variation was also computed using equation (7). For this computation, the antenna diameter of the TOPEX antenna was taken to be 1.292 meters [11]. The local elevation angle, which is measured from the satellite's local horizon up towards the local zenith, also varied over the contact time and was computed in radians. This elevation angle is the complement of the zenith angle measured in the STK simulations (subtract 90° from zenith angle in the simulations to obtain the local elevation angle).

The predicted variation in the received $(C/N_o)_r$ was based on the addition of the space loss and antenna pattern loss in dB units over time,

$$(C/N_o)_r = L_{sr}\,(dB) + L_p\,(dB) \quad (7)$$

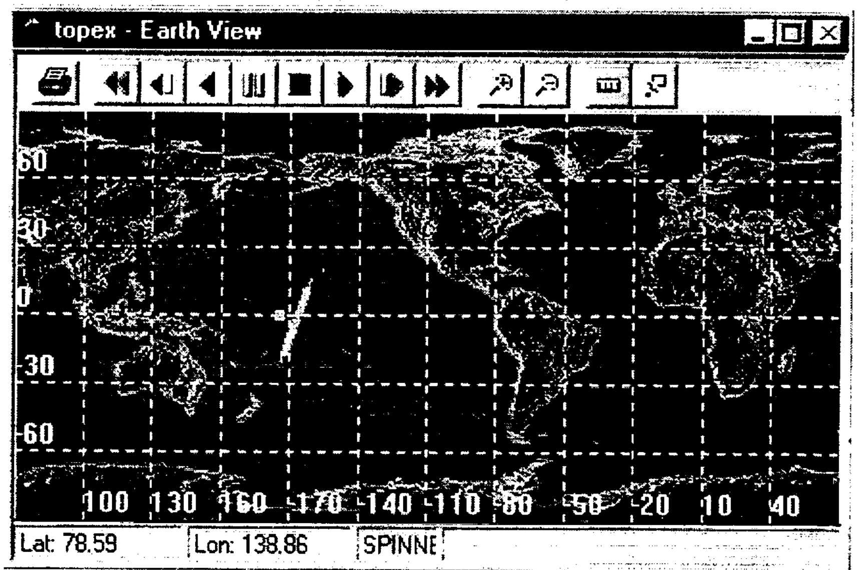

Figure 13. TOPEX Access to TDRS-W for Pass 1

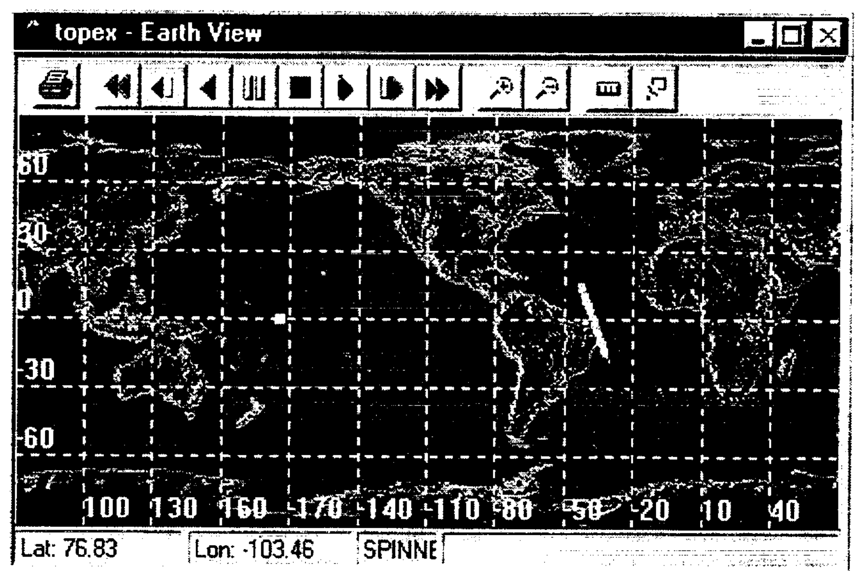

Figure 14. TOPEX Access to TDRS-E for Pass 2

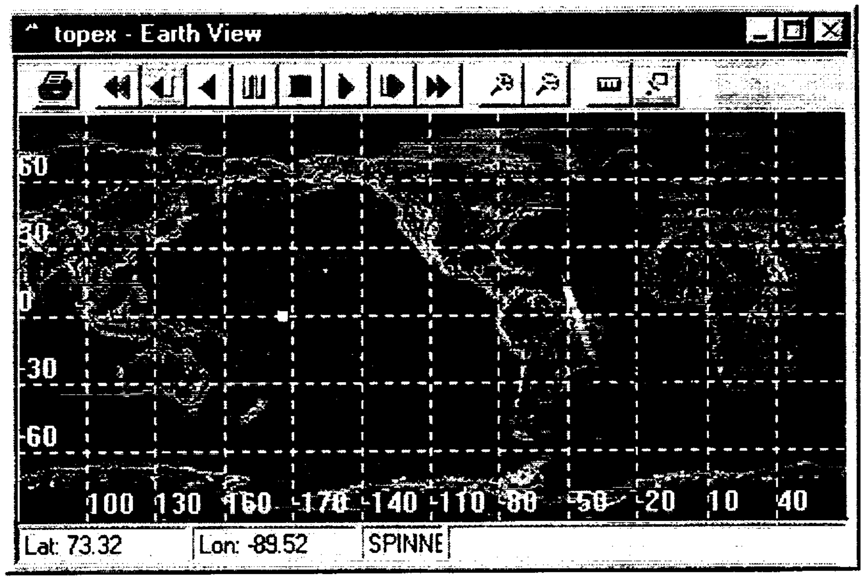

Figure 15. TOPEX Access to TDRS-E for Pass 3

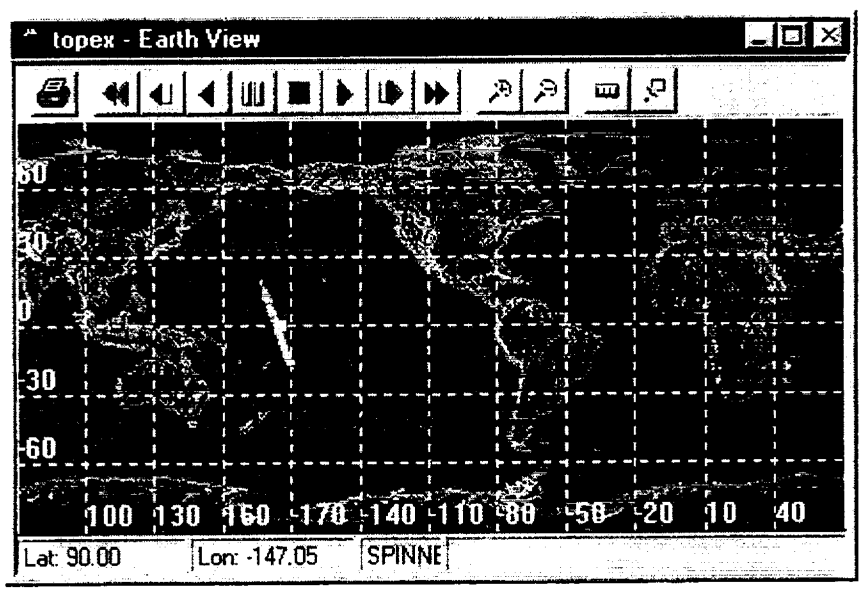

Figure 16. TOPEX Access to TDRS-W for Pass 4

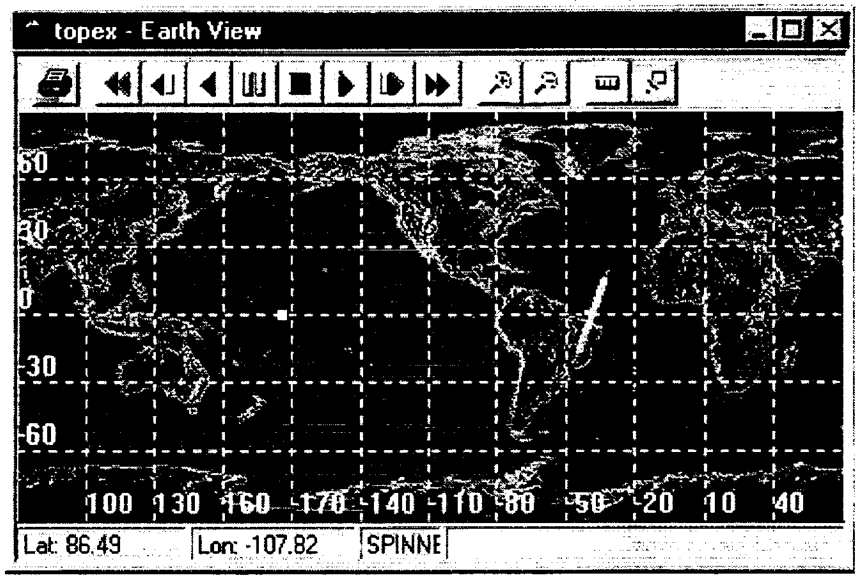

Figure 17. TOPEX Access to TDRS-E for Pass 5

Once the C/N_0 was computed and plotted from the simulation passes, the received signal strength was taken from the actual data and plotted on the same graphs for comparison. Figures 18 through 22 illustrate the relative gain vs. time for each of the five passes. The experimental data from the actual passes is indicated on the graphs with diamonds, while the data that was simulated and calculated is indicated with squares.

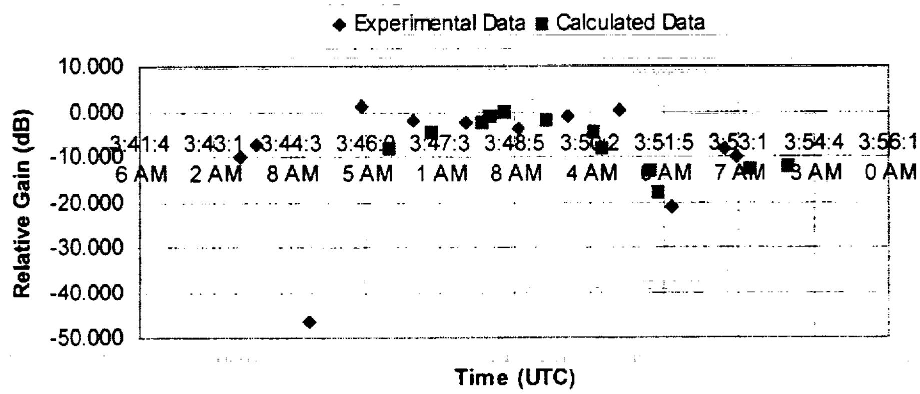

Figure 18. Comparison of Pass 1 - Day 174

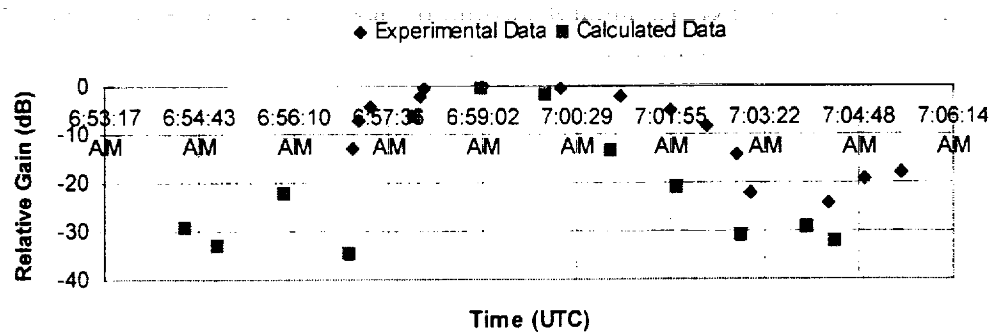

Figure 19. Comparison of Pass 2 - Day 175

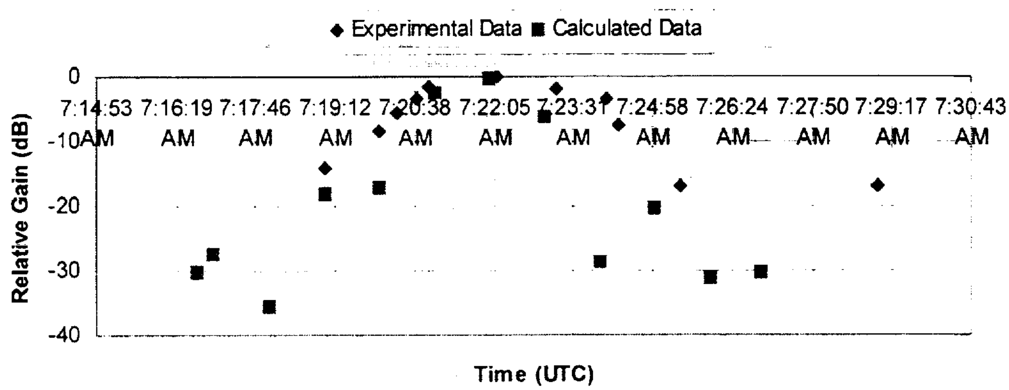

Figure 20. Comparison of Pass 3 - Day 176

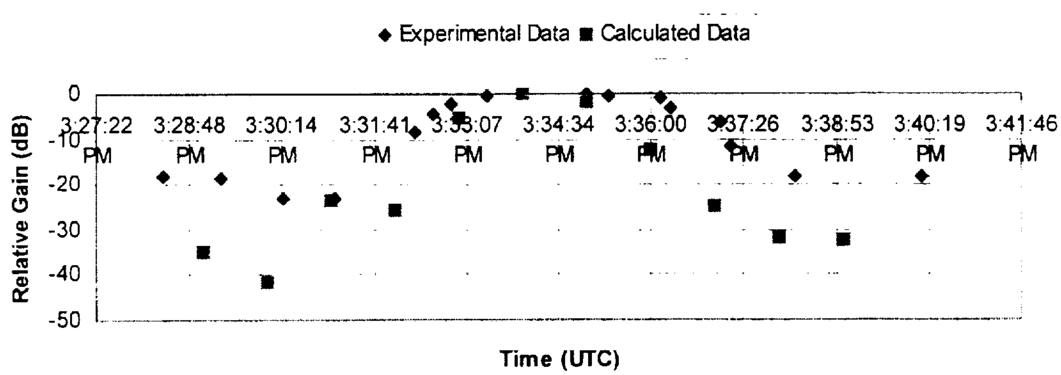

Figure 21. Comparison of Pass 4 - Day 178

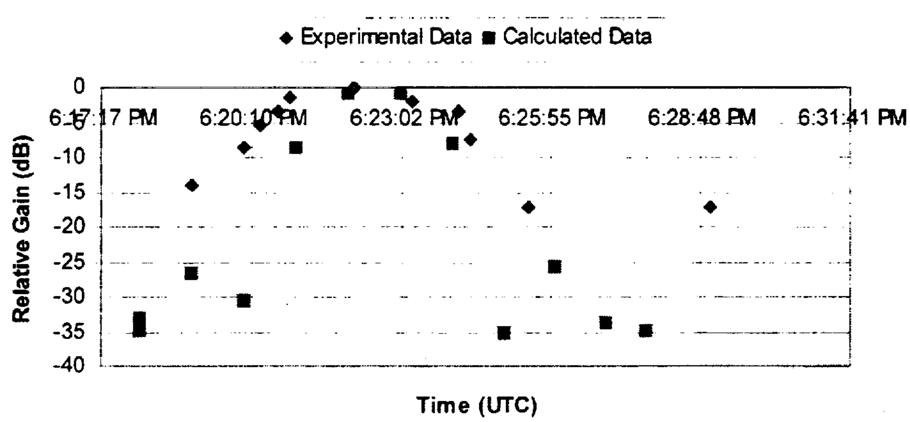

Figure 22. Comparison of Pass 5 - Day 178

CHAPTER 5 - ANALYSIS

We can estimate the total daily volume desired to be transmitted through the space network over the range of small satellite missions by considering that at the 50th percentile, NASA estimates that the daily data volume generated in these missions is equivalent to a continuous production rate of 10 kbps [12]. This corresponds to a total production of 864,000,000 bits per day (bpd). The required minimum data rate necessary to transport this desired data volume is a function of the contact duration per day. If we were to consider data volumes above the 50th percentile, the path loss and antenna gain differential results in approximately 35 dB power difference between data link to TDRS versus a ground station [13] would be expected to be too great to overcome. There are potential ways to overcome the 35 dB difference in link performance which include: increasing transmitter power, increasing antenna directivity, and data rate buffering. But we will be concentrating on the 50th percentile which should be able to afford the link penalty.

From Tables 3 through 6, the contact duration is listed as a function of inclination angle and half-angle for orbital altitudes of 600 km through 1200 km. The contact duration can therefore be used to calculate the required data rate for any particular model at the 50th percentile by

$$R_d\text{ (bps)} = \frac{\text{864,000,000 bpd}}{\text{Contact Duration (sec)}} \qquad (9)$$

The units on the data rate can be changed to *dBbps* by *10log(bps)*. Once the data rate is calculated, the Effective Isotropic Radiated Power that can be supported for each model can be calculated by

$$\text{EIRP (dbW)} = R_d + M - k - L_s - L_{pol} - L_{pnt} - L_{nc} - L_{rfi} \quad (10)$$

where R_d is the data rate, L_s is the space loss, L_{pol} is the antenna polarization loss, L_{pnt} is the antenna pointing loss, L_{nc} is the system noncompliance loss, and L_{rfi} is the RFI margin (*all losses and margins are in dB units*) [14]. The constant parameter K is a service specific value and equals 221.8 dB for a SN multiple access service with a worst-case bit error rate of 10^{-5} when the data is convolutionally coded with a standard rate ½ and constraint length 7 code (this a standard NASA communications configuration when using the SN) [15]. This analysis was also constrained by using the SMA communications service on the SN. This is the lowest performance communications service of the three service types available on the SN. The SSA communications service has the next highest performance level in the system. Referring back to equation (10), the service specific constant, K, is 230.7 dB for an SSA service vs. 221.8 dB for an SMA service. This difference of 8.9 dB implies that we have the potential to trade higher data rates, shorter access times, and system availability to achieve the optimum mission model by using both the SMA and SSA communications systems. To determine the maximum transmission rate possible, the assumption can be made that the link margin and the polarization, pointing, noncompliance, and RFI losses are 0 dB. The space loss is estimated using [16]

$$\text{Ls (dB)} = -(32.45 + 20\log(R) + 20\log(f)) \qquad (11)$$

where R is the slant range in Kilometers and f is the multiple access transmission frequency of 2287.5 MHz.

The slant ranges are listed in Table 9, corresponding to the half-angles of 10° through 40° that were examined. Only one inclination angle was used to determine the path length due to the fact that the antenna half-angles affect the slant ranges but not the inclinations angle. If the inclination angle was changed, with the same antenna half-angles, the slant ranges would be the same.

These relationships were used to generate a listing of Effective Isotropic Radiated Power (EIRP) as a function of expected data rates and slant ranges with the results given in Table 10 for an orbital altitude of 600-km for TDRS-West. Table 11 is given to illustrate the EIRP values for the full constellation which includes all TDRS satellites. From these tables, the 50th percentile level can be achieved by using either a wider half-angle and a single TRDS or a narrow half-angle antenna and the full constellation with a lower EIRP. TDRS-East and TDRS-ZOE yielded similar results so only TDRS-West is shown. In general, the narrow pointing angles require a higher EIRP than the broader pointing angles. This indicates that more power is needed for narrower HPBW antennas that are capable of supporting a relatively high data rate and only a few contacts with the SN which can be traded against a low-gain, broad HPBW antenna with low data rate and many contacts per day.

Typically, the gain for a small antenna is between 5 to 10 dB, thus, in this study, the gain is feasible between this constraint for the assumed 10 Watts of power transmitted. If the gain exceeds 10 dB, the small antenna is not realizable unless the

Table 9. Spin-Stabilized Satellite-to-TDRS Maximum Slant Paths				
	Orbital Altitude			
Pointing Half-Angle	600 km	800 km	1000 km	1200 km
10°	35283 km	35086 km	34887 km	34787 km
20°	35549 km	35357 km	35165 km	34972 km
30°	35987 km	35805 km	35622 km	35440 km
40°	36589 km	36422 km	36254 km	36086 km

Table 10. Effective Isotropic Radiated Power (EIRP) in dBW for *TDRS-W* at an Orbital Altitude of 600 km					
	Orbital Inclination				
Pointing Half-Angle	20°	40°	60°	80°	100°
10°	28.736	31.486	32.855	33.339	33.758
20°	22.346	25.476	26.829	27.48	27.371
30°	18.316	21.902	23.338	23.969	23.936
40°	16.736	19.241	20.859	21.496	21.533

Table 11. Effective Isotropic Radiated Power (EIRP) in dBW for *Full Constellation* at an Orbital Altitude of 600 km					
	Orbital Inclination				
Pointing Half-Angle	20°	40°	60°	80°	100°
10°	23.936	26.666	27.959	28.525	28.640
20°	17.543	20.616	21.951	22.559	22.551
30°	13.499	17.040	18.461	19.078	19.087
40°	11.899	14.387	15.986	16.629	16.660

frequency is large. The contact times for an individual TDRS or the entire SN constellation will need to be balanced against operations constraints.

CHAPTER 6 - CONCLUSIONS

From the simulations and analysis performed on the spin-stabilized satellite, it was determined that the lower gain antenna systems on the spin-stabilized satellite will allow for greater number of contacts per day but at a lower transmission rate, while the high gain antenna system allows few daily contacts at a higher transmission rate. The simulations also illustrated that the non-gimbaled antenna pointing had at least 3 contacts per day with existing technology or antennas that are readily available and up to 15 contacts per day with the correct choice of antenna and orbital inclination. The non-gimbaled antenna pointing gave sufficient contact time through the entire Space Network constellation to make this communication mode reasonable to investigate for actual usage. The technique provides approximately 15 minutes per day at the low end up through several hundred minutes at the high end with the duration being a function of the orbital inclination and antenna HPBW. The small orbital inclination angles or large antenna HPBW angles are needed to have large number of contact minutes per orbit and the narrower antenna has a small number of contact minutes per orbit and needs a large power gain. The simulations were run over a 30-day period to have a range variation.

Another set of simulations were run for the experimental satellite called TOPEX to verify pointing and simulation methodology using on actual satellite. The passes were determined from variations in the antennas near the subsatellite position of the TOPEX. Once the simulations were performed, the relative gain was calculated and plotted against the relative gain from the actual test data. These results showed that the simulation procedure was accurate. Since the simulation procedure was accurate for this case, we concluded that the spin-stabilized simulations previously performed would represent the performance of a real satellite.

Based on the simulation methodology and the experimental data received from JPL for the TOPEX satellite, this is an acceptable candidate for designing non-gimbaled antennas as a function of orbital inclination angles and various half-angles and a deviation of orbital altitudes.

Small satellite users can take advantage of the SN making comparable mission designs using the variation of parameters given in this study. The optimum mission model ultimately depends on the choice of TDRS to be used on a given data service depends on the relative satellite positions, the availability of the communications link, and the requested service duration.

REFERENCES

[1] National Aeronautics and Space Administration (NASA), Space Network (SN) Users' Guide, revision 6, Goddard Space Flight Center, September 1988, p. 1-1.

[2] NASA, ibid., p. 3-1.

[3] NASA, ibid., p. 3-22.

[4] Proakis, John, Digital Communications, 3rd ed., McGraw-Hill, p. 316, 1995.

[5] Proakis, John, ibid., p. 317.

[6] Ha, Tri., *Digital Satellite Communications*, 2nd ed., McGraw-Hill, p.80, 1990.

[7] Stutzman and Thiele, *Antenna Theory and Design*, Wiley, p. 421, 1981.

[8] Satellite Tool Kit, version 3, Analytical Graphics, King of Prussia, 1997.

[9] NORAD 2-Line Elements, available via anonymous ftp in the directory pub/space at archive.afit.af.mil.

[10] TOPEX picture, available via world wide web site: http:\\tethys.jpl.nasa.gov/images/newsat.gif.

[11] Pat Sanatar, Jet Propulsion Laboratory, private communication.

[12] Warner Miller, 1994, private communication.

[13] NASA, Communications and Data Systems Division.

[14] NASA, ibid., p. A-8.

[15] NASA, ibid., p. 3-24.

[16] NASA, ibid., p. A-3.